revista engenharia agrícola
Journal of the Brazilian Association of Agricultural Engineering
ISSN: 1809-4430 (on-line)

MODELLING HEAD LOSS ALONG EMITTING PIPES USING DIMENSIONAL ANALYSIS

Doi:http://dx.doi.org/10.1590/1809-4430-Eng.Agric.v35n3p442-457/2015

ACÁCIO PERBONI[1], JOSE A. FRIZZONE[2], ANTONIO P. DE CAMARGO[3], MARINALDO F. PINTO[4]

ABSTRACT: Local head losses must be considered in estimating properly the maximum length of drip irrigation laterals. The aim of this work was to develop a model based on dimensional analysis for calculating head loss along laterals accounting for in-line drippers. Several measurements were performed with 12 models of emitters to obtain the experimental data required for developing and assessing the model. Based on the Camargo & Sentelhas coefficient, the model presented an excellent result in terms of precision and accuracy on estimating head loss. The deviation between estimated and observed values of head loss increased according to the head loss and the maximum deviation reached 0.17 m. The maximum relative error was 33.75% and only 15% of the data set presented relative errors higher than 20%. Neglecting local head losses incurred a higher than estimated maximum lateral length of 19.48% for pressure-compensating drippers and 16.48% for non pressure-compensating drippers.

KEYWORDS: microirrigation, lateral line, maximum length.

MODELAGEM DA PERDA DE CARGA EM TUBOS EMISSORES USANDO ANÁLISE DIMENSIONAL

RESUMO: As perdas localizadas de carga nos emissores devem ser consideradas para cálculo preciso do comprimento máximo de linhas laterais de irrigação por gotejamento. O objetivo deste trabalho foi desenvolver um modelo utilizando análise dimensional para calcular perda de carga ao longo de linhas laterais de irrigação, constituídas por gotejadores *in-line*. Várias medições foram realizadas com 12 modelos de emissores a fim de obter dados experimentais requeridos para o ajuste e avaliação do modelo matemático. O modelo proposto foi classificado como excelente, de acordo com o coeficiente de Camargo & Sentelhas. Ocorreu aumento no desvio entre valores observados e estimados com o aumento da perda de carga, sendo que o desvio máximo foi de 0,17 m. O erro relativo máximo foi 33,73%, sendo que 15% dos dados ensaiados apresentaram erro relativo maior que 20%. A desconsideração da perda de carga localizada ocasionou superestimava do comprimento máximo da linha lateral de até 16,48%, para os tubos emissores não regulados, e de até 19,48%, para os tubos com emissores regulados.

PALAVRAS-CHAVE: microirrigação, linha lateral, comprimento máximo.

INTRODUCTION

The main objective of the trickle irrigation design is the uniform distribution of water delivered through the emitters (ZHU et al., 2010). Although drip irrigation systems have several advantages over other irrigation systems, the ideal water distribution along the lateral cannot be achieved due to variations in emitter discharge. These variations are influenced by operating pressure and water temperature (DOGAN & KIRNAK, 2010; BORSSOI et al., 2012); emitter

[1] Engenheiro Agrônomo, Doutorando, Departamento de Engenharia de Biossistemas, USP/Piracicaba – SP, Fone: (19) 3447-8576, acacio_perboni@yahoo.com.br
[2] Engenheiro Agrônomo, Prof. Titular, Departamento de Engenharia de Biossistemas, USP/Piracicaba – SP, frizzone@usp.br
[3] Engenheiro Agrônomo, Doutor, Instituto Nacional de Ciência e Tecnologia – Engenharia da Irrigação, USP/Piracicaba – SP, apcpires@usp.br
[4] Engenheiro Agrícola, Prof. Adjunto, Departamento de Engenharia, UFRRJ/Seropédica – RJ, marinaldopinto@usp.br
Recebido pelo Conselho Editorial em: 08-4-2013
Aprovado pelo Conselho Editorial em: 15-10-2014

manufacturing process; emitter clogging (TARCHITZKY et al., 2013; ZHOU et al., 2013) and pressure variations caused by slope (ZHU et al., 2010) and friction losses (RETTORE NETO et al., 2009; GOMES et al., 2010; VEKARIYA et al., 2011).

Total energy loss along laterals can be divided into two parts: major and minor losses. Major losses are associated with energy loss along the pipe due to frictional effects, which depend on fluid viscosity, wall roughness, internal diameter of the pipe, pipe length, and flow velocity. Although many equations are available for determining friction losses along laterals, the Darcy-Weisbach equation seems to be the most accepted for small diameter polyethylene pipes (YILDIRIM, 2009).

The introduction of the Blasius friction factor (equation 1) into the Darcy–Weisbach equation provides an accurate estimate of the frictional losses produced by turbulent flow inside uniform pipes with low wall roughness and when the Reynolds number (R) falls within the range 3,000-10^5 (CARRIÓN et al., 2013).

$$f = 0.316\ R^{-0.25} \tag{1}$$

For laminar flow regime ($R < 2000$), the friction factor f is given by [eq. (2)].

$$f = \frac{64}{R} \tag{2}$$

Low-density polyethylene is usually used in the manufacture of micro irrigation laterals. The internal diameter of polyethylene pipes is affected by operating pressure (JUANA et al., 2002), which can change the hydraulic conditions of an irrigation system.

RETTORE NETO (2011) presented a model for determining continuous head loss that considers the modulus of elasticity of material, wall thickness of pipe, pressure inside the pipe, and consequently internal diameter variation due to pressure effects (equation 3). According to the author, the equation was an improvement on the Darcy-Weisbach formula and presented excellent results in estimating continuous head loss of polyethylene pipes.

$$hf = f\ \frac{L}{\frac{D_t}{\left(1-\frac{P\ D_t}{e\ E}\right)}}\ \frac{V_t^2}{2\ g} \tag{3}$$

in which,

hf = head loss (m);

L = Pipe length (m);

D_t = internal diameter of the pipe (m);

V_t = mean water velocity at uniform pipe sections (m s^{-1});

g = gravitational acceleration (m s^{-2});

P = pressure inside the pipe (Pa);

e = wall thickness of pipe (m),

E = modulus of elasticity of material (Pa).

The insertion of emitters along a lateral line modifies the flow streamlines inducing additional pressure losses, which must be taken into consideration in order to accurately evaluate total energy losses along laterals (YILDIRIM, 2009).

The Borda-Carnot equation (equation 4) enables quantification of head losses caused by a sudden expansion or contraction along a pipeline:

$$hf_L = \frac{(V_e^2 - V_t^2)}{2\ g} = \left(1 - \frac{A_e}{A_t}\right)^2 \frac{V_t^2}{2\ g} \tag{4}$$

in which,

hf_L= local head loss (m);

V_e= water velocity at the section of flow contraction (m s^{-1});

A_e= cross-sectional area of flow where an emitter is located (m^2),

A_t= cross-sectional area of the pipe (m^2).

DEMIR et al. (2007) presented a model based on dimensional analysis to calculate the friction head loss in drip irrigation laterals equipped with in-line emitters (equation 5), which is valid for the following conditions: $0.2 \le S_e \le 1$ m; $0.01253 \le D_t \le 0.01377$ m; $0.01133 \le d \le 0.01205$ m; $0.03153 \le L_e \le 0.06868$ m; $3591 \le R \le 23688$.

$$\frac{\Delta H_S}{S_e} = 28.116 \left(\frac{V_t D_t}{v}\right)^{-0.771} \left(\frac{V_t^2}{g\ D_t}\right)^{1.248} \left(\frac{S_e}{D_t}\right)^{-0.258} \left(\frac{d}{D_t}\right)^{-3.008} \left(\frac{L_e}{d}\right)^{0.066} \tag{5}$$

in which,

ΔH_S = friction head loss between two consecutive emitters (m);

S_e = emitter spacing (m);

v = kinematic viscosity of water (m^2 s^{-1});

d = emitter inside diameter (m),

L_e = emitter length (m).

Dimensional analysis is a simple, clear and intuitive method for determining the functional dependence of physical quantities that influence a process (VEKARIYA et al., 2011). The aim of this work was to develop a model based on dimensional analysis for calculating head loss along laterals accounting for in-line drippers.

MATERIAL AND METHODS

Model development

Dimensional analysis is a useful tool for developing predictive equations, which reduces the physical quantities to dimensionless groups called Π terms (VEKARIYA et al., 2011). The Π theorem enables the organisation of experimental runs and the analysis of measurements by dimensionless groups. Using dimensionless groups permits a reduction in the number of runs and the testing of the global effects of the variables that occur in each group rather than the effect of each singular variable (FERRO, 2010).

In this study the term hf_{Se} was used to express the total head loss between two consecutive emitters. Using this approach, data analysis is easier to perform and the model becomes easier to operate. The proposed model considers that hf_{Se} is the sum of continuous and local head loss (equation 6). Continuous head loss between two consecutive emitters was expressed by the Darcy-Weisbach formula, in which the pipe length (L) was replaced with the distance between two consecutive emitters (S_e). Local head loss was calculated based on [eq. (4)], considering the mean cross-sectional area of flow where an emitter is located (Ae_m).

$$hf_{Se} = \left[f\,\frac{S_e}{D_t} + \left(1 - \frac{Ae_m}{A_t}\right)^2\right]\frac{V_t^2}{2\,g} \tag{6}$$

Equation (7) resulted from [eq. (6)] and it presents a theoretical model for estimating total head loss between two consecutive emitters, which considers the friction coefficient given by the Blasius equation (equation 1)] and the change in internal diameter due to elasticity and pressure inside the pipe (equation 3).

$$hf_{Se} = \left\{\left[0.316\left(\frac{V_t D_t}{v}\right)^{-0,25}\frac{S_e\left(1 - \frac{P\,D_t}{e\,E}\right)}{D_t}\right] + \left(1 - \frac{Ae_m}{A_t}\right)^2\right\}\frac{V_t^2}{2g} \tag{7}$$

The following relationship can therefore be defined:

$$hf_{Se} = \text{Ø}(V_t, D_t, v, S_e, g, P, e, E, Ae_m, A_t) \tag{8}$$

in which,

Ø is a functional symbol.

Table 1 presents [eq. (8)] rewritten as a dimensional matrix.

TABLE 1. Dimensional matrix.

	hf_{Se}	V_t	D_t	v	S_e	P	e	E	g	A_t	Ae_m
M	0	0	0	0	0	1	0	1	0	0	0
L	1	1	1	2	1	1	-1	-1	1	2	2
T	0	-1	0	-1	0	-2	0	-2	-2	0	0

Table 1 shows eleven variables, where hf_{Se} is the dependent variable and the remainder are independent variables ($V_t, D_t, v, S_e, P, e, E, g, A_t, Ae_m$). The physical process involves three dimensions (M, L, and T) and eight Π terms. The basic selected variables were V_t, D_t and P because they are dimensionally independent. The Π terms shown in Table 2 were obtained by applying the Vaschy-Buckingham theorem.

TABLE 2. Dimensionless terms.

Dimensionless term		Meaning
Π term	Function	
Π_1	$\frac{hf_{Se}}{D_t}$	Relationship between head loss and pipe diameter
Π_2	$\frac{v}{V_t D_t}$	Inverse of Reynolds number
Π_3	$\frac{S_e}{D_t}$	Relationship between distance of emitters and pipe diameter
Π_4	$\frac{g D_t}{V_t^2}$	Inverse of Froude number
Π_5	$\frac{A_t}{D_t^2}$	Relationship between cross-sectional area of the pipe and the square of the pipe diameter
Π_6	$\frac{Ae_m}{D_t^2}$	Relationship between mean cross-sectional area of flow where an emitter is located and the square of the pipe diameter
Π_7	$\frac{e}{D_t}$	Relationship between wall thickness and pipe diameter
Π_8	$\frac{E}{P}$	Relationship between modulus of elasticity and pressure inside the pipe

The first dimensionless term was obtained by combining hf_{Se} with the three basic variables (equation 9).

$$\Pi_1 = hf_{Se}\, P^{\alpha 1} V_t^{\alpha 2} D_t^{\alpha 3} \tag{9}$$

Rewriting [eq. (9)] as a dimensional equation:

$$(MLT)^0 = L^1\, (M^1 L^{-1} T^{-2})^{\alpha 1} (L^1 T^{-1})^{\alpha 2}\, (L^1)^{\alpha 3} \tag{10}$$

The exponents of each dimension in [eq. (10)] are: $\alpha 1 = 0, \alpha 2 = 0, \alpha 3 = -1$, and consequently the first Π term (equation 11) was obtained by substituting these values into [eq. (9)].

$$\Pi_1 = hf_{Se}\, D_t^{-1} \tag{11}$$

The second Π term was determined by combining v with the basic variables and the other dimensionless terms were also obtained by a similar process.

Equation (12) was determined considering $\Pi_1 = \emptyset(\Pi_2, \Pi_3, \Pi_4, \Pi_5, \Pi_6, \Pi_7, \Pi_8)$. The terms Π_5 and Π_6 were grouped into a single term ($\frac{Ae_m}{A_t}$).

$$\frac{hf_{Se}}{D_t} = \varnothing\left(\frac{V_t D_t}{\nu}, \frac{S_e}{D_t}, \frac{V_t^2}{gD_t}, \frac{Ae_m}{A_t}, \frac{e}{D_t}, \frac{E}{P}\right) \tag{12}$$

Since Π terms were defined, 816 measurements were performed with 12 models of cylindrical in-line drippers to obtain the experimental data required for developing and assessing the model. Seventy percent of the collected data was applied to model developing and 30% was applied to model assessment and validation.

Model assessment and validation

The Camargo & Sentelhas coefficient (CAMARGO & SENTELHAS, 1997) was used to indicate the model performance at estimating head loss. This coefficient combines the accuracy and precision of a model in a single value (equation 15) that can be interpreted based on Table 3. The Camargo & Sentelhas coefficient is the product of Pearson's correlation coefficient (equation 13) and Willmott's index of agreement (equation 14).

$$r = \frac{\sum_{i=1}^{n}[(x_i - \bar{x})(y_i - \bar{y})]}{\sqrt{\sum_{i=1}^{n}(x_i - \bar{x})^2}\sqrt{\sum_{i=1}^{n}(y_i - \bar{y})^2}} \tag{13}$$

$$I_d = 1 - \frac{\sum_{i=1}^{n}(y_i - x_i)^2}{\sum_{i=1}^{n}(|y_i - \bar{x}| + |x_i - \bar{x}|)^2} \tag{14}$$

$$c = r\, I_d \tag{15}$$

in which,

x = observed values;

y = estimated values;

r = Pearson's correlation coefficient;

I_d = Willmott's index of agreement,

c = the Camargo & Sentelhas coefficient.

TABLE 3. Criteria for interpreting model performance based on the Camargo & Sentelhas coefficient (CAMARGO & SENTELHAS, 1997).

c	Performance
> 0.85	Excellent
0.76 - 0.85	Very good
0.66 - 0.75	Good
0.61 - 0.65	Regular
0.51 - 0.60	Unsatisfactory
0.41 - 0.50	Bad
≤ 0.40	Awful

Testing conditions

The research was carried out at the Irrigation Laboratory of the Department of Biosystems Engineering, University of São Paulo, Piracicaba, Brazil. The tests were performed in a closed circuit system (FIGURE 1) consisting of: a water tank; a centrifugal pump; three valves for controlling pressure and flow rate; an electromagnetic flowmeter (range 0 to 1500 Lh^{-1}, accuracy ±0.5%); a digital manometer (range 0 to 1470 kPa, accuracy ±0.25%) and a mercury differential manometer able to measure a maximum value of 266.65 kPa.

The differential manometer was used to determine total head loss along the lateral. Emitting pipes/emitters were totally plugged before carrying out the experiments and four repetitions were performed on each model. The pressure at the lateral inlet during all the tests was 196 kPa (±0.98 kPa) and the flow rate ranged from 160 to 1420 Lh^{-1} in increments of 80 Lh^{-1}.

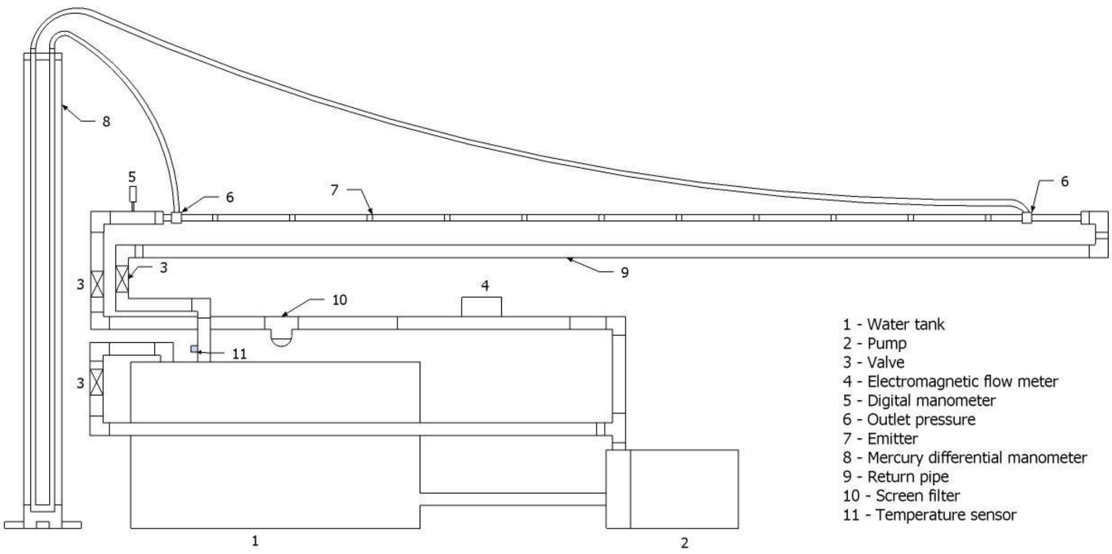

FIGURE 1. Diagram of the facility used to perform the tests.

For each emitting pipe model, the internal diameter (D_t) and wall thickness (e) of eight samples were measured using a horizontal benchtop optical comparator Starret HB400. The cross-sectional area of the pipe (A_t) and the flow velocity at the pipe section (V_t) were determined based on measured values of D_t.

A digital thermometer (resolution 0.01ºC) was used to measure water temperature during the tests in order to estimate the kinematic viscosity and density of the water.

Following the procedure described by RETTORE NETO (2011), a tensile test machine (FIGURE 2) was used to perform uniaxial tensile tests in order to determine the modulus of elasticity of the pipes. Three repetitions were performed for each model of emitting pipe. The tested samples were 25-cm lengths and the machine was configured to apply tension at a speed of 10 mm/minute.

FIGURE 2. Tensile test machine used to determine modulus of elasticity of polyethylene pipes.

Methodology for determining the cross-sectional area of flow where an emitter is located

The mean cross-sectional area of flow where an emitter is located (Ae_m) was determined indirectly based on the volume of distilled water required to fill up a cylinder of pipe in which the emitter was assembled. Eight samples (cylinders) were extracted from each model of emitting pipe.

The length of each sample was exactly the length occupied by an emitter inside the pipe. The samples were sealed at one side so that they could be filled with water. Empty and water-filled samples were weighed using a digital balance (resolution 0.01 g). The value Ae_m of each sample was obtained by dividing the water volume inside each cylinder by its length. A digital caliper (resolution 0.01 mm) was used to measure the cylinder length.

RESULTS AND DISCUSSION

Model input data

Table 4 and 5 describe the geometric properties of the pipes and emitters evaluated during the experiments.

TABLE 4. Properties of the pipes evaluated during the experiments.

Emitting pipe	L (m)	Internal diameter (mm)		Wall thickness (mm)		E (MPa)
		$\bar{x}$	σ	$\bar{x}$	σ	$\bar{x}$
1	9.80	13.60	0.15	1.18	0.06	102.86
2	10.14	13.91	0.22	1.12	0.03	125.68
3	9.90	13.75	0.07	1.11	0.06	114.88
4	10.40	13.57	0.16	1.30	0.05	95.43
5	10.50	13.65	0.23	1.16	0.03	104.47
6	10.36	13.49	0.18	0.81	0.03	137.93
7	10.27	15.01	0.17	1.14	0.07	104.29
8	10.36	15.22	0.17	1.06	0.05	103.94
9	10.40	17.12	0.24	1.22	0.04	98.67
10	10.20	15.67	0.37	1.00	0.05	124.37
11	10.40	14.28	0.30	1.15	0.08	113.48
12	10.50	17.30	0.39	1.20	0.13	115.43

$\bar{x}$ = average; σ = standard deviation;

The standard deviation values of Ae_m shown in Table 5 represent manufacturing differences between samples of the same model of emitter. The highest coefficient of variation among the tested models was 2.02% (emitter 6) and such a low value seems to be sufficient to support the feasibility of using this methodology. Moreover, this methodology allows easy and rapid determination of Ae_m and requires no sophisticated equipment.

TABLE 5. Properties of the emitters evaluated during the experiments.

Emitter	Picture	N	S_e (m)	Relation pressure-flow rate $q_{(Lh^{-1})} = Kh^{x}_{(kPa)}$		L_e (mm)		Ae_m (mm²)	
				k	x	$\bar{x}$	σ	$\bar{x}$	σ
1		10	0.98	2.048	0.064	34.34	0.05	108.74	2.13
2		13	0.78	2.592	-0.027	35.94	0.07	105.10	1.91
3		11	0.90	3.994	0.001	50.04	0.14	109.35	2.06
4		20	0.52	1.518	0.092	34.22	0.07	107.45	2.04
5*	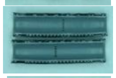	21	0.50	0.045	0.625	68.15	0.04	110.01	1.45
6		14	0.74	2.722	-0.017	35.86	0.07	105.76	2.14
7		13	0.79	1.659	0.046	37.39	0.08	135.97	2.47
8		14	0.74	3.380	-0.043	36.03	0.09	137.03	1.90
9*		52	0.20	0.106	0.500	39.59	0.07	197.97	1.64
10*		17	0.60	0.132	0.520	32.06	0.05	191.46	1.76
11	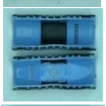	26	0.40	1.650	0.038	48.87	0.09	187.94	1.57
12	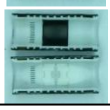	35	0.30	0.644	0.072	48.84	0.10	189.96	1.64

N = Number of emitters along the lateral; k and x = coefficients of the pressure-flow rate function; * = non pressure-compensating drippers.

Validation and assessment of the model

As mentioned previously, 70% of the gathered data was applied to fitting the model coefficients by multiple linear regression. The statistical results related to this procedure are shown in Table 6.

TABLE 6. Statistical analysis.

Statistical parameter			
R multiple	R^2 adjusted	Standard error	Number of measurements
0.9951	0.9901	0.0629	571

ANOVA						
Source of variation	DF	SQ	QM	F	F_{tab}(1%)	F_{sig}
Regression	4	225.484	56.371	14256.808	3.05	0
Error	566	2.238	0.004			
Total	570	227.722				

DF = degrees of freedom; SQ = Sum of squares; QM = Mean of squares; F = Calculated value of F-Test statistic; F_{tab} = Critical value of the F distribution at α = 0.01; F_{sig} = Significance level of acceptance of the null hypothesis.

The calculated value of F was higher than the critical value and therefore the hypothesis of regression existence was accepted. The adjusted coefficients were evaluated by t-test and all of them differed from zero considering a significance level of 1% (Table 7).

TABLE 7 - Regression coefficients.

Term	Regression coefficients	Standard deviation	t-test	Value of P	Confidence interval (95%)		R^2
					Lower	Upper	partial
constant	-0.880	0.062	-14.229	<0.0001	-1.002	-0.759	-
$\frac{E}{P}$	-	-	-0.742	0.4580	-	-	0.00013
$\frac{e}{D_t}$	0.466	0.050	9.408	<0.0001	0.369	0.563	0.00154
$\frac{V_t^2}{D_t g}$	0.909	0.005	190.715	0	0.899	0.918	0.85200
$\frac{V_t D_t}{v}$	-	-	-	-	-	-	0.00034
$\frac{Ae_m}{A_t}$	-1.452	0.046	-31.403	<0.0001	-1.543	-1.361	0.01850
$\frac{S_e}{D_t}$	0.790	0.014	57.298	0	0.763	0.817	0.11800

t_{tab} (1%) = 2.58; Value of P = Significance level of acceptance of the hypothesis that the regression exponent is equal to zero.

Since the Reynolds number and Froude number presented collinearity, the Reynolds number was removed from the analysis because this term presented low statistical correlation with the dependent variable. With a Reynolds number higher than 10,000, BAGARELLO et al. (1997) observed that local head losses are not influenced by the Reynolds number and only depend on emitter geometry. JUANA et al. (2002) also mentioned that, in practice, the effects of viscous forces on the coefficient of local head loss are negligible beyond a limiting value of Reynolds number. The $E\,P^{-1}$ term was also removed because it is only meaningful within the significance level of 45.85%. The testing pressure during all experiments was 196 kPa (±0.98 kPa). Perhaps if other testing pressures were evaluated during experiments, this term could have presented a higher significance level. Nevertheless, both removed terms presented low values of partial R^2 and have practically no effect on the model (Table 7).

[eq. (16)] was determined by substituting the regression coefficients from Table 7 into [eq. (12)] and applying the anti-logarithm.

$$\frac{hf_{Se}}{D_t} = 0.13179\left(\frac{V_t D_t}{\upsilon}\right)^{0}\left(\frac{S_e}{D_t}\right)^{0.79}\left(\frac{V_t^2}{gD_t}\right)^{0.909}\left(\frac{Ae_m}{A_t}\right)^{-1.452}\left(\frac{e}{D_t}\right)^{0.466}\left(\frac{E}{P}\right)^{0} \tag{16}$$

Finally, after replacing A_t with D_t, assuming g is equal to 9.81 m s^{-2}, and rearranging the terms, the proposed model is given by [eq. (17)].

$$hf_{Se} = 0.01164\,\frac{S_e^{0.79}}{D_t^{-1.739}}\,\frac{V_t^{1.818}}{Ae_m^{1.452}}\,e^{0.466} \tag{17}$$

The model is valid for emitting pipes considering the following attributes and thresholds: $0.2 \le S_e \le 0.98$ m; $0.01349 \le D_t \le 0.01730$ m; $0.18 \le V_t \le 2.8$ m s^{-1}; $0.105\times10^{-3} \le Ae_m \le 0.198\times10^{-3}$ m^2.

The proposed model can be classified as excellent, based on the obtained value of the Camargo & Sentelhas coefficient equal to 0.9925 (CAMARGO & SENTELHAS, 1997).

According to Figure 3A, the spread of data increased proportionally to the head loss. DEMIR et al. (2007) observed the same behavior studying drip irrigation laterals equipped with in-line and on-line emitters. The maximum error (ϵ) between observed and estimated values of head loss was 0.17 m (Figure 3A). Considering 816 measurements, Figure 3B shows that only 15% of the data set presented a relative error higher than 20%, whereas the maximum value was 33.73%. Since only a single equation was used to estimate head losses in several models of emitting pipes, the relative errors varied between emitting pipes due to their inherent differences. PROVENZANO & PUMO (2004) also reported significant differences among investigated dripline models. Relative errors increased according to head loss for all emitting pipes except pipe 9. Differences in relative errors between repetitions were observed and might be caused by experimental errors. Emitting pipes 5, 9 and 12 presented the highest values of relative error (Figure 3C).

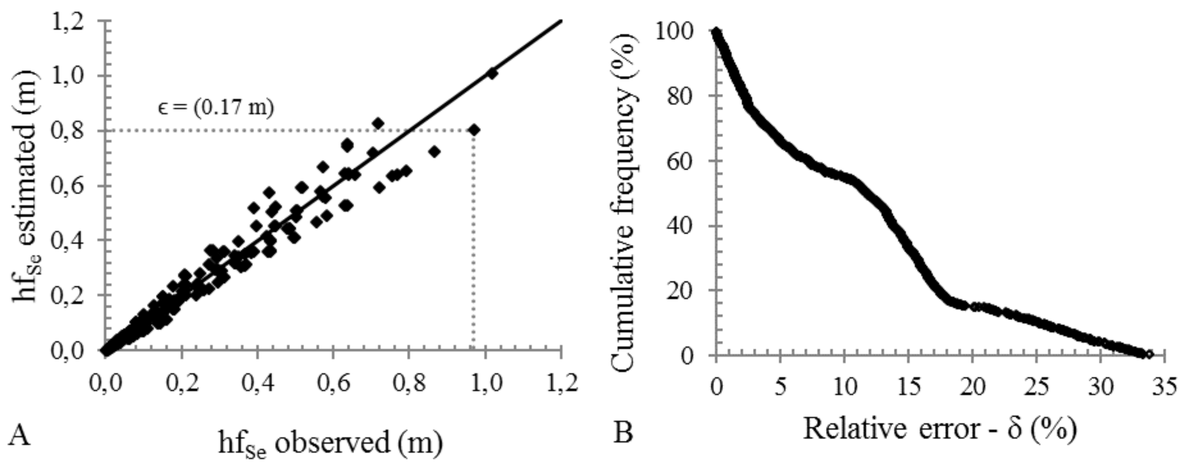

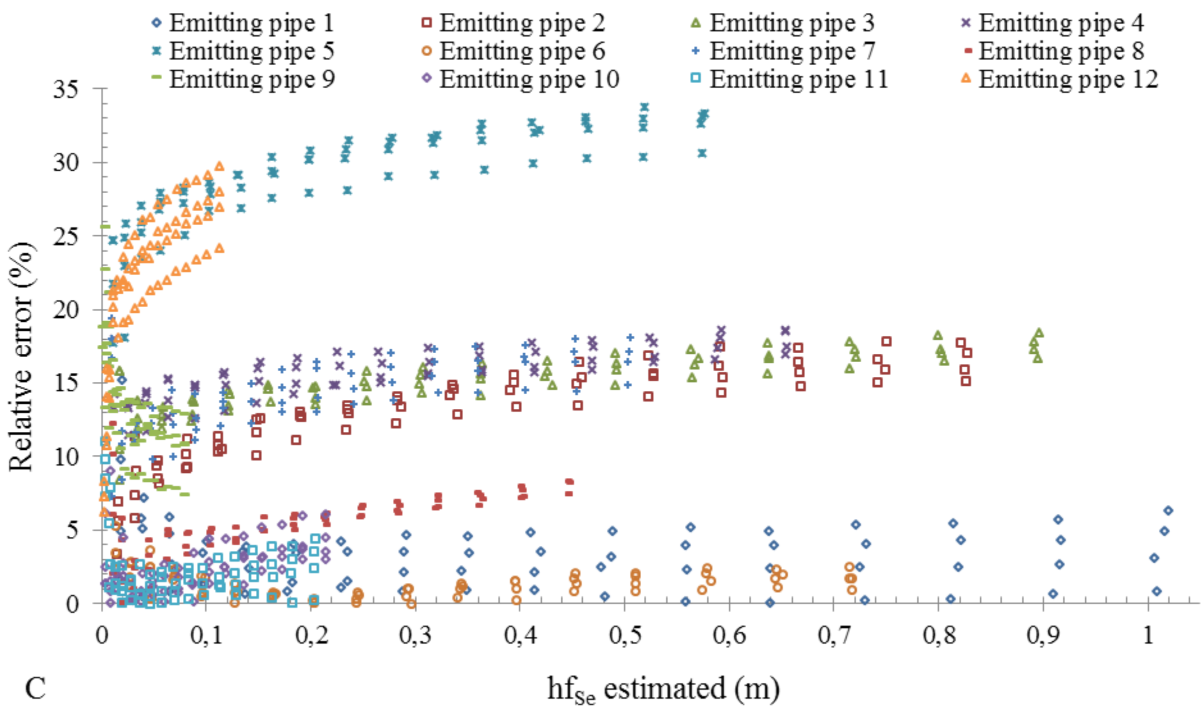

FIGURE 3. A) Estimated versus observed values of head loss; B) Cumulative frequency versus relative error on estimating head loss ($\delta = 100\left|\frac{hf_{Se_{observed}} - hf_{Se_{estimated}}}{hf_{Se_{observed}}}\right|$); C) Relative error versus hf_{Se} estimated for individual emitting pipes.

Comparison between the proposed model and the model presented by DEMIR et al. (2007)

The model presented by DEMIR et al. (2007) can be applied to estimating the head loss of just 5 of the 12 emitting pipes studied in this research (emitting pipes 1, 3, 4, 5, and 6). Figure 4 groups charts presenting observed hf_{Se}, estimated hf_{Se} by the proposed model and estimated hf_{Se} using the model presented by DEMIR et al. (2007). Comparing both models, the proposed model presented estimated hf_{Se} closer to the observed values for all emitting pipes, except pipe 5.

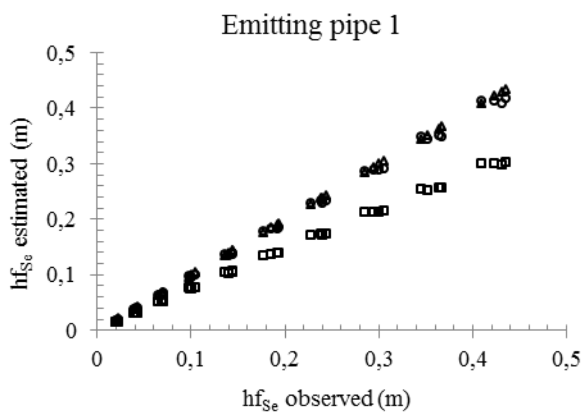

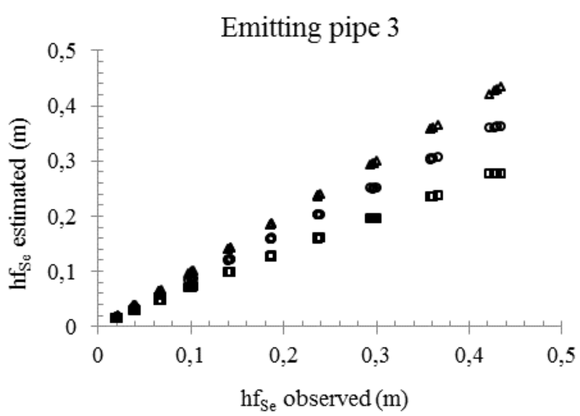

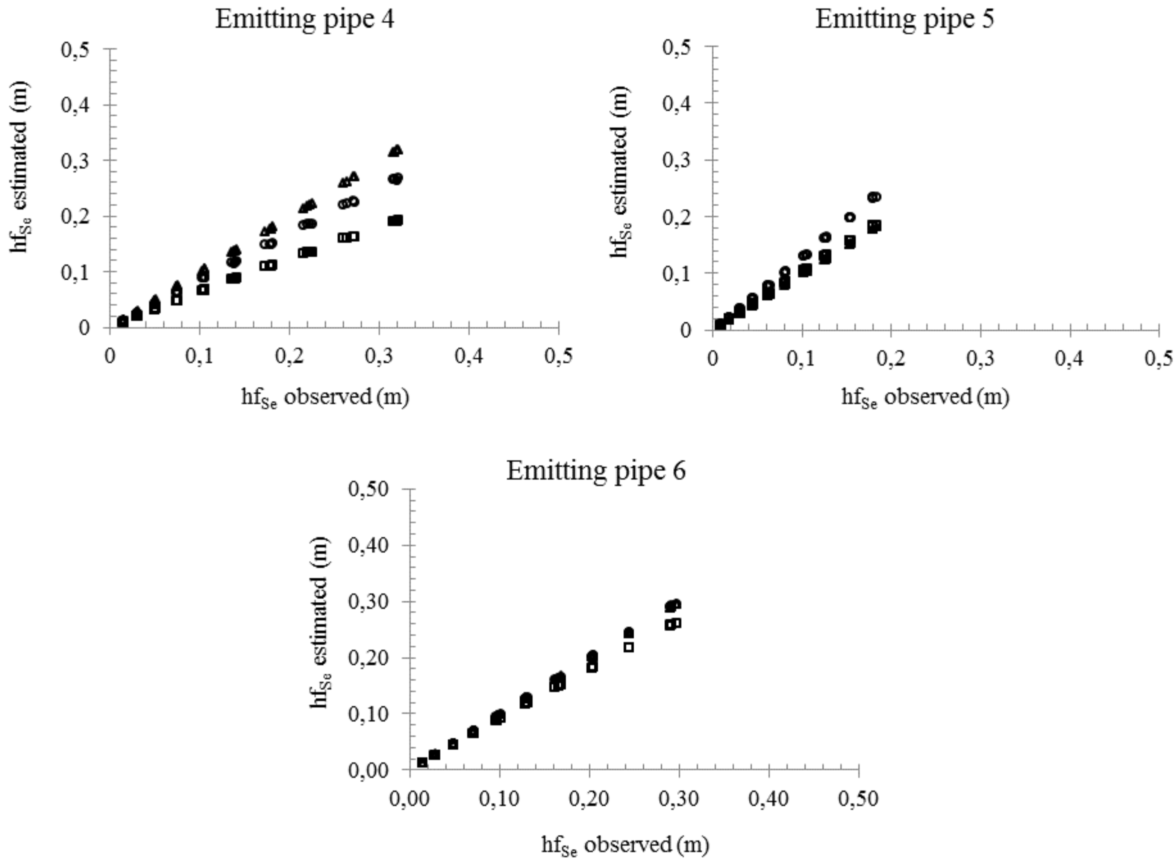

FIGURE 4. Observed hf$_{Se}$(Δ), estimated hf$_{Se}$ by the proposed model (○), and estimated hf$_{Se}$ using the model presented by DEMIR et al. (2007) (□).

Applying the developed model on designing laterals

An example of how to apply the developed model on designing the maximum length of laterals is presented and it assumes the following criteria: a) the maximum flow velocity along the lateral is 1.5 m s^{-1}; b) the allowable variation in emitters' flow rate along the lateral is 5% and c) pressure at the lateral inlet is 120 and 200 kPa for non pressure-compensating (NPC) and pressure-compensating (PC) emitters, respectively.

The maximum length of 12 models of emitting pipes was simulated by two methods. The first one was a step-by-step method based on the Darcy-Weisbach equation that does not take into account local head loss effects (a), whereas the second refers to the model developed in this study (b). The maximum length of the laterals and the difference between the values obtained from both methods are summarised in Table 8.

TABLE 8. Maximum length of laterals placed on a level ground.

Emitting pipe	hf_{adm} (m)	A	B	100 (A-B)/A
		L_{max}(m)	L_{max}(m)	ΔL_{max}(%)
1	10.2	208	180	13.46
2	10.2	211	175	17.06
3	10.2	158	136	13.92
4	10.2	154	124	19.48
5*	0.92	122	105	13.93
6	10.2	183	164	10.38
7	10.2	260	226	13.08
8	10.2	212	183	13.68
9*	1.14	91	76	16.48
10*	1.1	128	130	-1.56
11	10.2	159	162	-1.89
12	10.2	303	248	18.15

L_{max} = maximum lateral length (m); hf_{adm} = allowable head loss (m); A = results neglecting local head loss effects; B = results provided by the developed model; ΔL_{max} = difference in maximum lateral length between A and B; * = non pressure-compensating drippers.

Comparing results from both methods, ΔL_{max} gave a value of 19.48%, which seems to represent a significant difference caused by neglecting local head loss effects. Depending on the type of dripper, GOMES et al. (2010) reported that maximum lateral length could be overestimated by around 25.7% (NPC drippers) and 9.5% (PC drippers) when local head losses were neglected. Based on the results shown in Table 8, the maximum lateral length was overestimated by around 19.48% (emitting pipe 4 - PC dripper) and 16.48% (emitting pipe 9 - NPC dripper) when local head losses were neglected.

CONCLUSIONS

The model developed for estimating total head loss along drip irrigation laterals requires only the following parameters: distance between emitters (S_e); internal diameter (D_t) and wall thickness (e) of the pipe; flow velocity (V_t) and mean cross-sectional area of flow where an emitter is located (Ae_m). Although the final parameter (Ae_m) is not available in the manufacturer's catalogue, the methodology presented in this work enables easy and rapid determination of Ae_m and requires no sophisticated equipment.

Based on the Camargo & Sentelhas coefficient, the model for estimating head loss was classified as excellent and can be applied to the design of laterals accounting for in-line cylindrical emitters. Only 15% of the data set presented relative errors higher than 20%, whereas the maximum value was 33.73%. Since a single equation was used to estimate head losses, relative errors varied between emitting pipes due to their inherent peculiarities. Relative errors increased according to head loss for most of the emitting pipes.

The maximum lateral length was overestimated by around 19.48% for PC drippers and 16.48% for NPC drippers when local head losses were neglected.

ACKNOWLEDGEMENTS

The authors are grateful to NaanDanJain for supplying the emitting pipes used in this research, as well as the following Brazilian institutions for their financial support: the Federal Department of Science and Technology (MCT); the National Scientific and Technological

Development Council (CNPq); the Sao Paulo State Scientific Foundation (FAPESP) and the National Institute of Science and Technology in Irrigation Engineering (INCTEI).

REFERENCES

BAGARELLO, V.; FERRO, V.; PROVENZANO, G.; PUMO, D. Evaluating pressure losses in drip--irrigation lines. **Journal of Irrigation and Drainage Engineering**, New York, v. 123, n. 1, p. 1-7, 1997.

BORSSOI, A. L.; VILAS BOAS, M. A.; REISDÖRFER, M.; HERNÁNDEZ, R.; FOLLADOR, F. A. C. Water application uniformity and fertigation in a dripping irrigation set. **Engenharia Agrícola**, Jaboticabal, v. 32, n.4, p. 718-726, 2012.

CAMARGO, A. P; SENTELHAS, P. C. Avaliação do desempenho de diferentes métodos de estimativa da evapotranspiração potencial no estado de São Paulo, Brasil. **Revista Brasileira de Agrometeorologia**, Santa Maria, v. 5, n. 1, p. 89-97, 1997.

CARRIÓN, F.; TARJUELO, D.; HERNÁNDEZ, D.; MORENO, M. A. Design of microirrigation subunit of minimum cost with proper operation. **Irrigation Science**, New York, p. 1-9, 2013. doi: http://dx.doi.org/10.1007/s00271-013-0399-8.

DEMIR, V.; YURDEM, H.; DEGIRMENCIOGLU, A. Development of prediction models for friction losses in drip irrigation laterals equipped with integrated in-line and on-line emitters using dimensional analysis. **Biosystems Engineering**, Silsoe, v. 96, n. 4, p. 617-631, 2007.

DOGAN, E.; KIRNAK, H. Water temperature and system pressure effect on drip lateral properties. **Irrigation Science**, New York, v. 28, n. 5, p. 407-419, jun. 2010.

FERRO, V. Deducing the USLE mathematical structure by dimensional analysis and self-similarity theory. **Biosystems Engineering**, Silsoe, v. 106, n. 2 , p. 216-220, 2010.

GOMES, A. W. A.; FRIZZONE, J. A.; RETTORE NETO, O.; MIRANDA, J. H. Perda de carga localizada em gotejadores integrados em tubos de polietileno. **Engenharia Agrícola**, Jaboticabal, v. 30, n.3, p. 435-446, 2010.

JUANA, L.; RODRÍGUES-SINOBAS, L.; LOSADA, A. Determining minor head losses in drip irrigation laterals: I - Methology. **Journal of Irrigation and Drainage Engineering**, New York, v. 128, n. 6, p. 376-384, 2002.

PROVENZANO, G.; PUMO, D. Experimental analysis of local pressure losses for microirrigation laterals. **Journal of Irrigation and Drainage Engineering**, New York, v. 130, n. 4, p. 318-324, 2004.

RETTORE NETO, O. **Modelo para determinação da perda de carga em tubos elásticos**. 2011. 95 f. Tese (Doutorado em Irrigação e Drenagem) – Escola Superior de Agricultura "Luiz de Queiroz", Universidade de São Paulo, Piracicaba, 2011.

RETTORE NETO, O.; FRIZZONE, J. A.; MIRANDA, J. H; BOTREL, T. A. Perda de carga localizada em emissores não coaxiais integrados a tubos de polietileno. **Engenharia Agrícola**, Jaboticabal, v. 29, n.1, p. 28-39, 2009.

TARCHITZKY, J.; RIMON, A.; KENIG, E.; DOSORETZ, C. G.; CHEN, Y. Biological and chemical fouling in drip irrigation systems utilizing treated wastewater. **Irrigation Science**, New York, v. 31, n. 6, p. 1277-1288, 2013.

VEKARIYA, P. B.; SUBBAIAH, R.; MASHRU, H. H. Hydraulics of microtube emitters: a dimensional analysis approach. **Irrigation Science**, New York, v. 29, n. 4, p. 341-350, 2011.

YILDIRIM, G. Simplified procedure for hydraulic design of small-diameter plastic pipes. **Irrigation and Drainage**, New York, v. 58, n. 2, p. 209-233, 2009.

ZHOU, B.; L, Y.; PEI, Y.; LIU, Y.; ZHANG, Z.; JIANG. Y. Quantitative relationship between biofilms components and emitter clogging under reclaimed water drip irrigation. **Irrigation Science**, New York, p. 1-13, 2013. doi: http://dx.doi.org/ 10.1007/s00271-013-0402-4.

ZHU, D. L.; WU, P. T.; MERKLEY, G. P.; JIN, J. Drip irrigation lateral design procedure based on emission uniformity and field microtopography. **Irrigation and Drainage**, New York, v. 59, n. 5, p. 535-546, 2010.